

Spectroscopic Identification of Transition-Metal $M[\eta^2-(O,O)C]$ Species for Highly-Efficient CO_2 Activation

Huijun Zheng,[#] Xiangtao Kong,[#] Chong Wang, Tiantong Wang, Dong Yang, Gang Li, Hua Xie, Zhi Zhao,^{*} Ruili Shi, Haiyan Han, Hongjun Fan,^{*} Xueming Yang, and Ling Jiang^{*}



Cite This: *J. Phys. Chem. Lett.* 2021, 12, 472–477



Read Online

ACCESS |



Metrics & More

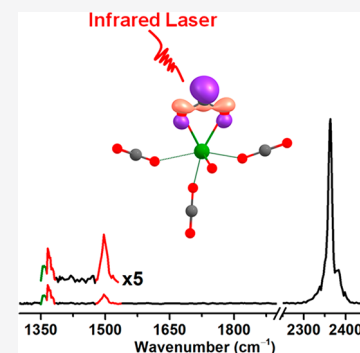


Article Recommendations



Supporting Information

ABSTRACT: The CO_2 activation by transition metals is important in CO_2 utilization but has proven to be challenging for experimental targets. Here we report first synthesis and spectroscopic characterization of transition-metal $M[\eta^2-(O,O)C]$ species with bidentate double oxygen metal- CO_2 coordination in the $[ZrO(CO_2)_{n \geq 4}]^+$ complexes. The $Zr[\eta^2-(O,O)C]$ species yields a CO_2^- radical ligand, showing a high efficiency in CO_2 activation. We find that two important prerequisites are demanded for certain metals to form this intriguing $M[\eta^2-(O,O)C]$ species. One is that the metal center has high reduction capability, and the other is that the oxidation state of the metal center is lower than its highest one by 1. This study highlights the pivotal roles played by the $M[\eta^2-(O,O)C]$ species in CO_2 activation and also open new avenues toward the development of related single-atom catalysts with isolated transition-metal atoms dispersed on supports.



The atmospheric concentration of carbon dioxide (CO_2) has risen significantly over the past century, which has imposed severe consequences for global climate change and planetary temperature increase.^{1–3} The capture and utilization of CO_2 to create valuable chemicals is highly desired with regard to reducing CO_2 from the atmosphere and using CO_2 as a feedstock for sustainable energy sources.^{1,2} As a central role in the processes of CO_2 utilization, CO_2 activation has been proven to be an important yet challenging target because of the high bond dissociation energy and ionization potential of CO_2 . The interaction of CO_2 with metal complexes plays a vital role in the activation and reduction of the robust CO_2 molecule.^{4–12} Spectroscopic studies of mass-selected metal complexes help uncover the microscopic mechanism of single-atom catalysis processes at the molecular level.^{13–17}

The coordination mode of CO_2 to the metal provides crucial information in understanding the degree of CO_2 activation and the structure–reactivity relationship of metal– CO_2 complexes.⁹ There are four potential binding motifs for the coordination of a single CO_2 to a single metal center, $M(\eta^1-OCO)$, $M(\eta^1-CO_2)$, $M[\eta^2-(C,O)O]$, and $M[\eta^2-(O,O)C]$.⁹ Carbonate and oxalate motifs involve more complicated ligands, with more than one CO_2 molecule or the exotic oxygen atom. The $M(\eta^1-OCO)$ binding motif denotes a $M \cdots O=C=O$ structure and is dominated in most mononuclear metal– CO_2 cations, in which the antisymmetric CO stretch of CO_2 is typically blue-shifted by 20–30 cm^{-1} from the corresponding mode of free CO_2 at 2349 cm^{-1} , indicating a weak interaction between CO_2 and metal center.^{18–27} The $M(\eta^1-CO_2)$ and $M[\eta^2-(C,O)O]$ motifs are common in the anionic and neutral mononuclear metal– CO_2 complexes, in

which the antisymmetric CO stretch of CO_2 appears in the 1600–1900 cm^{-1} region, reflecting the expected weakening of the CO bonds.^{5,28–34} The antisymmetric CO stretch of CO_2 in an $M[\eta^2-(O,O)C]$ motif ($M = Li, Na, K, Rb, Cs, Mg$) is below 1600 cm^{-1} , largely red-shifted by more than 750 cm^{-1} with respect to free CO_2 , signifying a substantial activation of CO_2 .⁹

The $M[\eta^2-(O,O)C]$ species is proposed to be highly reactive due to the lone pair/unpaired electron on the carbon atom and could be an intermediate state in the formation of C–C bonds.⁹ Thus, the $M[\eta^2-(O,O)C]$ motif is significantly important in the CO_2 activation and utilization. However, experimental characterization of the $M[\eta^2-(O,O)C]$ motif has been very challenging, with only a few successful infrared (IR) spectroscopic studies in several alkali and alkaline earth metal– CO_2 complexes.^{35–39} Here, we present the synthesis and characterization of an unprecedented transition-metal $M[\eta^2-(O,O)C]$ motif in the mononuclear $ZrO-CO_2$ complexes in the form of $[ZrO(CO_2)_{n \geq 4}]^+$. The resulting $Zr[\eta^2-(O,O)C]$ moiety harvests a CO_2^- radical ligand and signifies a high efficiency in CO_2 activation.

The $[ZrO(CO_2)_n]^+$ complexes were prepared and characterized by an infrared photodissociation (IRPD) spectroscopy apparatus described previously (see Experimental method in

Received: November 12, 2020

Accepted: December 17, 2020

the Supporting Information).⁴⁰ The $[\text{ZrO}(\text{CO}_2)_n]^+$ complexes were produced by pulsed laser vaporization of a zirconium target in a supersonic expansion of 100% CO_2 . Figure S1 shows the mass spectra obtained at the experimental conditions that favor the formation of $[\text{ZrO}(\text{CO}_2)_n]^+$ complexes with relatively high thermodynamic stability. The energy of IR photons from the table-top LaserVision system is not sufficient to cause efficient dissociation of the $[\text{ZrO}(\text{CO}_2)_n]^+$ ($n = 1$ and 2) complexes (Table S1). The messenger tagging efficiency of $[\text{ZrO}(\text{CO}_2)_n]^+$ is too low to allow the present IRPD measurement. The $[\text{ZrO}(\text{CO}_2)_3]^+$ complex dissociates via loss of CO_2 after IR photoexcitation in the 2300–2400 cm^{-1} region but not in the 1300–1900 cm^{-1} region, whose absence could be due to either the number of photons required to dissociate coupled with the low IR pulse energy or the structural uncertainty (see Figure S2 for the details). Starting at $n = 4$, the fragmentation is observed in both regions. Infrared spectra were obtained by monitoring the fragment ions as a function of the IR photodissociation laser wavelength and normalized by parent ion signal and IR laser pulse energy.

The experimental IR spectra of $[\text{ZrO}(\text{CO}_2)_n]^+$ ($n = 4-7$) complexes are shown in the left column of Figure 1, and the

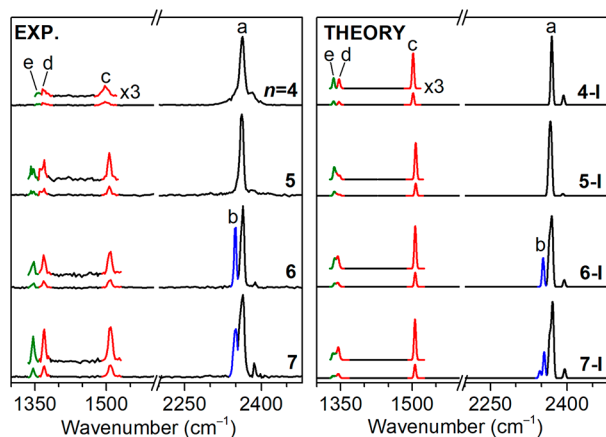


Figure 1. Comparison of the experimental and calculated IR spectra of $[\text{ZrO}(\text{CO}_2)_n]^+$ ($n = 4-7$).

band positions are listed in Table 1. Five features (labeled a–e in Figure 1) are resolved in the IR spectra. Band a presents in all the clusters studied here and slightly blue-shifts from 2363 to 2366 cm^{-1} upon addition of the CO_2 molecules. Band a is assigned to the antisymmetric CO stretch of weakly bound

CO_2 in the first coordination sphere.⁹ Band b appears as a shoulder at $n = 6$ and is retained in the $n = 7$ cluster, which can be assigned to the antisymmetric CO stretch of weakly bound CO_2 in the second or larger coordination sphere.⁹ Bands c and d are observed in the 1350–1550 cm^{-1} region for $n = 4-7$, which are characteristic of the antisymmetric and symmetric CO stretches of CO_2 in an $\text{M}[\eta^2-(\text{O},\text{O})\text{C}]$ motif.^{9,35–38} Band e appears as a small shoulder at 1354 cm^{-1} for $n = 4$ and gains in intensity for the larger clusters, which is attributed to the characteristic Fermi resonance of CO_2 arising from anharmonic coupling between the symmetric stretch vibration and the overtone of the bending mode as reported recently.²⁷

Quantum chemical calculations support the aforementioned assignment and provide detailed insights into the electronic structures of $[\text{ZrO}(\text{CO}_2)_n]^+$ (see Theoretical method in the Supporting Information). The structures were optimized by B3LYP hybrid functional augmented with a dispersion correction (B3LYP-D) together with the def2-TZVPP basis set. The possible structural motifs reported previously⁹ were considered in the present calculations, which lead to the location of three types of structures as illustrated in Figure S3. The quartet $[\text{ZrO}(\text{CO}_2)_n]^+$ isomers were found to be much higher in energy than the corresponding doublet isomers. Accordingly, only the results obtained for the isomers with the doublet ground electronic state are shown here. The lowest-energy structures (labeled n -I) identified for $[\text{ZrO}(\text{CO}_2)_n]^+$ ($n = 4-7$) are illustrated in Figure 2, in which each cluster consists of an $\text{Zr}[\eta^2-(\text{O},\text{O})\text{C}]$ motif with the formation of two metal–oxygen bonds between CO_2 and a single metal center. Figure 1 shows the comparison of experimental spectra of $[\text{ZrO}(\text{CO}_2)_n]^+$ ($n = 4-7$) and calculated spectra of n -I isomers.

In the calculated IR spectrum of isomer 4-I (Figure 1, trace 4-I), the main antisymmetric CO stretching vibrational frequency of weakly bound CO_2 is predicted to be 2370 cm^{-1} (Table 1), which is consistent with the experimental value of 2363 cm^{-1} . The calculated band c (1502 cm^{-1}) and d (1347 cm^{-1}) is attributed to the antisymmetric and symmetric CO stretches of CO_2 in the $\text{Zr}[\eta^2-(\text{O},\text{O})\text{C}]$ moiety, respectively, which agree with the experimental values (1497 and 1366 cm^{-1}). The characteristic Fermi resonance of CO_2 (band e) has been recently discussed in detail.²⁷ The calculated IR spectra of the lowest-energy isomers for the $n = 5-7$ clusters also agree well with the experimental spectra. In addition to bands a, c, d, and e, a feature near 2350 cm^{-1} (band b) in the $n = 6$ cluster is predicted in the simulated IR spectrum of isomer 6-I (Figure 1, trace 6-I), which is assigned

Table 1. Experimental Band Positions (cm^{-1}), Calculated Scaled Harmonic Vibrational Frequencies of the n -I Isomers, and Band Assignments for $[\text{ZrO}(\text{CO}_2)_n]^+$ ($n = 4-7$)

		$n = 4$	$n = 5$	$n = 6$	$n = 7$	assignment
band a	exp.	2363	2362	2364	2366	antisymmetric CO stretch of weakly bound CO_2 in the first coordination sphere
	theory	2370	2367	2370	2371	
band b	exp.	–	–	2350	2352	antisymmetric CO stretch of weakly bound CO_2 in the second coordination sphere
	theory	–	–	2353	2355	
band c	exp.	1497	1506	1509	1509	antisymmetric CO stretch of CO_2 in the $\text{Zr}[\eta^2-(\text{O},\text{O})\text{C}]$ motif
	theory	1502	1507	1506	1506	
band d	exp.	1366	1370	1368	1370	symmetric CO stretch of CO_2 in the $\text{Zr}[\eta^2-(\text{O},\text{O})\text{C}]$ motif
	theory	1347	1348	1344	1345	
band e	exp.	1354	1342	1348	1346	Fermi resonance of CO_2 arising from anharmonic coupling between the symmetric stretch vibration and the overtone of the bending mode
	theory	1335	1337	1338	1334	

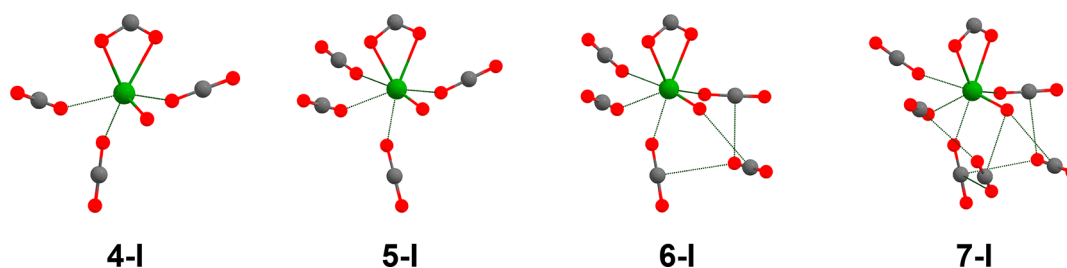


Figure 2. Identified structures of $[\text{ZrO}(\text{CO}_2)_n]^+$ ($n = 4-7$) (Zr, green; C, gray; O, red).

to the asymmetric CO stretch of weakly bound CO_2 in the second solvation shell. The agreement of the calculated spectra with experiment is reasonable to confirm the assignment of the n -I ($n = 4-7$) isomers responsible for the experimental spectra. The calculated spectra of energetically higher isomers n -II ($M(\eta^1\text{-OCO})$) and n -III ($M(\eta^2\text{-carbonate})$) are discrepant from experiment (Figures S4–S7). The barriers for the conversion from isomers n -II to isomers n -I ($n = 4-7$) are about 22–37 kJ/mol at the B3LYP-D/def2-TZVPP level of theory (Table S2), supporting the observation of isomers n -I with relatively high thermodynamic stability.

The observation of a bidentate double oxygen $\text{Zr}[\eta^2\text{-(O,O)C}]$ motif is quite interesting because such binding mode implies substantial activation of CO_2 , providing the first experimental evidence for the formation of $M[\eta^2\text{-(O,O)C}]$ motif in a transition-metal complex. Originally, the $\eta^2\text{-(O,O)C}$ motif has been only established in alkali and alkaline earth- CO_2 complexes ($M = \text{Li, Na, K, Rb, Cs, Mg}$), which are suggested to benefit from the high oxophilicity of the metals.^{35–38} Recent infrared multiple photon dissociation (IRMPD) spectroscopic studies of the $[\text{MgCO}_2(\text{H}_2\text{O})_n]^+$ clusters indicate that three H_2O molecules are necessary to induce charge transfer from a Mg^{2+} center to a CO_2 ligand.³⁹

Computational studies were carried out to study the detailed properties of transition-metal $M[\eta^2\text{-(O,O)C}]$ motifs, including the electronic structure, stability, and the formation conditions. The detailed structures and relative energies are shown in Figures S8–S13. There are two possible electronic structures for the $\eta^2\text{-(O,O)C}$ motif. One is the CO_2^- radical ligand as exemplified in alkali metal- CO_2 complexes,^{35,36} and the other is the CO_2^{2-} carbene ligand as illustrated in alkaline earth metal- CO_2 complexes.^{37,38} The singly occupied molecular orbital (SOMO) of $[\text{ZrO}(\text{CO}_2)_4]^+$ is shown in Figure 3, which strongly suggests that the $\eta^2\text{-(O,O)C}$ motif is a CO_2^- radical ligand. The calculated spin densities (C 0.724, O 0.108) and natural charges (C 0.82, O -0.66) also support the characterization of CO_2^- radical ligand. This is not surprising

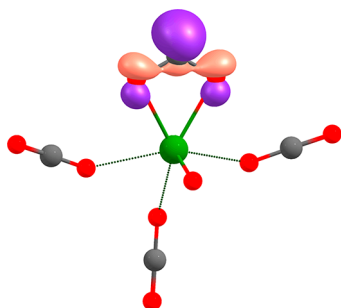


Figure 3. Singly occupied molecular orbital depiction of $[\text{ZrO}(\text{CO}_2)_4]^+$ (Zr, green; C, gray; O, red).

since the oxidation state of Zr in $[\text{ZrO}]^+$ core is +3, and only one valence electron is left and can be transferred to CO_2 . In contrast, the formation of common $M(\eta^1\text{-OCO})$ binding mode does not require electron transfer from metal to CO_2 , whereas the formation of $M(\eta^1\text{-CO}_2)$ and $M[\eta^2\text{-(C,O)O}]$ binding modes involves double electron transfer from metal to CO_2 . Further complete active space self-consistent field (CASSCF) calculation with 14 orbitals and 17 electrons in the active space (which includes most frontier σ/π orbitals of $\eta^2\text{-(O,O)C}$, d orbitals of Zr, and p orbitals of terminal oxo) confirms that the $[\text{ZrO}(\text{CO}_2)_4]^+$ complex does not have notable multireference character. Time-dependent density functional theory (TD-DFT) calculations at the B3LYP-D/def2-TZVPP level of theory indicate that the first three excited states are SOMO to $\eta^2\text{-(O,O)C}$ (π^*), SOMO to Zr(d), and SOMO to Zr(d), with the excitation energies of 3.94, 4.18, and 4.26 eV, respectively. These calculations further support our assignment of the CO_2^- radical ligand in $[\text{ZrO}(\text{CO}_2)_4]^+$.

Since the $\eta^2\text{-(O,O)C}$ motif in $[\text{ZrO}(\text{CO}_2)_4]^+$ is the one electron reduction product of CO_2 achieved by the Zr^{3+} , the reduction capability of Zr^{3+} could be crucial for the stability of $\eta^2\text{-(O,O)C}$ motif. The $\eta^1\text{-OCO}$ coordination of CO_2 molecules donate electrons to the transition metal⁴¹ and increases reduction capability of the Zr^{3+} . Therefore, the formation of $\eta^2\text{-(O,O)C}$ motif shall benefit from the additional $\eta^1\text{-OCO}$ coordination to the Zr^{3+} center. This explains why the $\eta^1\text{-OCO}$ motif is energetically favored in the $[\text{ZrO}(\text{CO}_2)_n]^+$ ($n = 1$ and 2) complexes and the $\eta^2\text{-(O,O)C}$ motif is preferred in the $n \geq 3$ complexes (Figure S3). Furthermore, the energy difference of the $\eta^2\text{-(O,O)C}$ and $\eta^1\text{-OCO}$ coordination increases smoothly from $n = 3$ to 7. In contrast, for the $[\text{HfO}(\text{CO}_2)_n]^+$ complexes, our computational experiments suggest that two CO_2 molecules are able to induce the conversion of $\text{Hf}(\eta^1\text{-OCO})$ to $\text{Hf}[\eta^2\text{-(O,O)C}]$ motif (Figure S8). This implies that the $\text{Hf}[\eta^2\text{-(O,O)C}]$ motif is easier to be formed than $\text{Zr}[\eta^2\text{-(O,O)C}]$, which is consistent with a stronger reduction capability of Hf than Zr. With this context, the Ti metal has a weaker reduction capability than Zr, and the $\text{Ti}[\eta^2\text{-(O,O)C}]$ motif should be much less energetically favorable, which is corroborated by our calculations of the $[\text{TiO}(\text{CO}_2)_n]^+$ complexes (Figure S9). Indeed, the CO_2 keeps $\eta^1\text{-OCO}$ coordination even for $n = 6$ in the $[\text{TiO}(\text{CO}_2)_n]^+$ system (Figure S9). Further computational experiments indicate that single electron transfer for the formation of $\eta^2\text{-(O,O)C}$ motif is overwhelmingly dominated in the $\text{Y}^{\text{II}}\text{O}(\text{CO}_2)_4$ and $[\text{Y}^{\text{II}}\text{Cl}(\text{CO}_2)_4]^+$ complexes (Figure S10b), but not in the $[\text{Nb}^{\text{IV}}\text{N}(\text{CO}_2)_4]^+$ complex in which Nb has a weaker reduction capability (Figure S11). For the K metal with very high reduction capability, the formation of the $\text{K}[\eta^2\text{-(O,O)C}]$ motif is undoubtedly preferred (Figure S12), which is consistent with its successful observation in the argon and

nitrogen matrices.³⁶ These results indicate that, in contrast with the η^1 -OCO coordination, the η^2 -(O,O)C motif is only preferred when the reduction capability of the metal center is pretty high. As expected, the η^2 -(O,O)C coordination is completely unstable in the $[\text{Y}^{\text{III}}\text{O}(\text{CO}_2)_4]^+$ complexes where no electron transfer is available (Figure S10a).

The CO_2 coordination with double electron transfer general exists in transition-metal complexes with high reduction capability. In the $[\text{Zr}(\text{CO}_2)_n]^+$ and $[\text{ZrO}(\text{CO}_2)_n]$ systems with double electrons available for transfer from Zr to CO_2 (Figure S13b), our calculations indicate the η^2 -(O,O)C motif is energetically unfavorable, implying that single electron transfer for the formation of CO_2^- is less competitive than double electron transfer for the formation of OZrCO^+ and/or $\text{C}_2\text{O}_4^{2-}$. As a result, the transition-metal $\text{M}[\eta^2$ -(O,O)C] motif is supposed to be only preferred when double electron transfer is not available. Thus, it can be referred that the formation of transition-metal $\text{M}[\eta^2$ -(O,O)C] motif is just favored when the oxidation state of the metal is lower than its highest oxidation state by 1 (for example, Y^{II} , La^{II} , Zr^{III} , Hf^{III} , etc.).

Based on the above discussions, the η^2 -(O,O)C motif in transition-metal complex signifies a CO_2^- radical ligand. Two conditions are required for the formation of η^2 -(O,O)C motif: the metal center has high reduction capability, and the oxidation state of metal center is lower than its highest oxidation state by 1. This could be the reason why the transition-metal $\text{M}[\eta^2$ -(O,O)C] motif has not been observed in previous studies. In general, the neutral and negative transition-metal complexes have higher reduction capability than the corresponding cations; therefore, such $\text{M}[\eta^2$ -(O,O)C] motif might also be formed in some neutral and negative transition-metal systems that meet the aforementioned two prerequisites.

In summary, the novel $[\text{ZrO}(\text{CO}_2)_{n \geq 4}]^+$ complexes exhibit a distinctive $\text{Zr}[\eta^2$ -(O,O)C] motif, in which both oxygen atoms are bounded to a single-metal-atom center. This intriguing $\text{Zr}[\eta^2$ -(O,O)C] motif shows a high efficiency in CO_2 activation. We find that two conditions are required for certain metals to form a specific $\text{M}[\eta^2$ -(O,O)C] motif. One is the metal center has high reduction capability and the other is the oxidation state of the metal center is lower than its highest one by 1. Our study indicates that the $\text{M}[\eta^2$ -(O,O)C] motif can also be created in the $\text{Hf}-\text{CO}_2$ and $\text{Y}-\text{CO}_2$ complexes and is thus suggested to be a widely existed binding mode for CO_2 activation in transition-metal complexes. The CO_2^- radical and nonlinear character of these series of $\text{M}[\eta^2$ -(O,O)C] complexes may enable high reactivity in many important reactions such as C-C coupling, C-H activation, etc. Systematic analyses for the effects of different transition and main-group metals on the formation of $\text{M}[\eta^2$ -(O,O)C] complexes provide comprehensive insights into the microscopic mechanism of CO_2 activation by a single metal center, offering design criteria for single-atom catalyst with isolated transition-metal atoms dispersed on supports. Such advances may be integrated into the CO_2 -activation and -utilization technology.

■ ASSOCIATED CONTENT

SI Supporting Information

The Supporting Information is available free of charge at <https://pubs.acs.org/doi/10.1021/acs.jpcllett.0c03379>.

Experimental and theoretical methods, Figures S1–S13, Tables S1 and S2, and references (PDF)

■ AUTHOR INFORMATION

Corresponding Authors

Zhi Zhao – School of Mathematics and Physics, Hebei University of Engineering, Handan 056038, China; Email: zhaozhi@hebeu.edu.cn

Hongjun Fan – State Key Laboratory of Molecular Reaction Dynamics, Dalian Institute of Chemical Physics, Chinese Academy of Sciences, Dalian 116023, China; orcid.org/0000-0003-3406-6932; Email: fanhj@dicp.ac.cn

Ling Jiang – State Key Laboratory of Molecular Reaction Dynamics, Dalian Institute of Chemical Physics, Chinese Academy of Sciences, Dalian 116023, China; orcid.org/0000-0002-8485-8893; Email: ljjiang@dicp.ac.cn

Authors

Huijun Zheng – State Key Laboratory of Molecular Reaction Dynamics, Dalian Institute of Chemical Physics, Chinese Academy of Sciences, Dalian 116023, China; University of Chinese Academy of Sciences, Beijing 100049, China; orcid.org/0000-0003-2876-7580

Xiangtao Kong – College of Chemistry and Chemical Engineering, Anyang Normal University, Anyang 455000, China

Chong Wang – State Key Laboratory of Molecular Reaction Dynamics, Dalian Institute of Chemical Physics, Chinese Academy of Sciences, Dalian 116023, China; University of Chinese Academy of Sciences, Beijing 100049, China

Tiantong Wang – State Key Laboratory of Molecular Reaction Dynamics, Dalian Institute of Chemical Physics, Chinese Academy of Sciences, Dalian 116023, China; University of Chinese Academy of Sciences, Beijing 100049, China

Dong Yang – State Key Laboratory of Molecular Reaction Dynamics, Dalian Institute of Chemical Physics, Chinese Academy of Sciences, Dalian 116023, China

Gang Li – State Key Laboratory of Molecular Reaction Dynamics, Dalian Institute of Chemical Physics, Chinese Academy of Sciences, Dalian 116023, China

Hua Xie – State Key Laboratory of Molecular Reaction Dynamics, Dalian Institute of Chemical Physics, Chinese Academy of Sciences, Dalian 116023, China; orcid.org/0000-0003-2091-6457

Ruili Shi – School of Mathematics and Physics, Hebei University of Engineering, Handan 056038, China

Haiyan Han – School of Mathematics and Physics, Hebei University of Engineering, Handan 056038, China

Xueming Yang – State Key Laboratory of Molecular Reaction Dynamics, Dalian Institute of Chemical Physics, Chinese Academy of Sciences, Dalian 116023, China; Department of Chemistry, Southern University of Science and Technology, Shenzhen 518055, China; orcid.org/0000-0001-6684-9187

Complete contact information is available at: <https://pubs.acs.org/10.1021/acs.jpcllett.0c03379>

Author Contributions

#H. Z. and X. K. contributed equally to this work.

Notes

The authors declare no competing financial interest.

ACKNOWLEDGMENTS

This work was supported by the National Natural Science Foundation of China (21327901, 21688102, 21673224, 21873097, 21976049, 12004094, and 12004095), the Strategic Priority Research Program of the Chinese Academy of Sciences (CAS) (XDB17000000), Dalian Institute of Chemical Physics (DICP DCLS201701 and DCLS201702), International Partnership Program of CAS (121421KYSB20170012), CAS (GJJSTD20190002), and K. C. Wong Education Foundation (GJTD-2018-06).

REFERENCES

- (1) Hepburn, C.; Adlen, E.; Beddington, J.; Carter, E. A.; Fuss, S.; Mac Dowell, N.; Minx, J. C.; Smith, P.; Williams, C. K. The Technological and Economic Prospects for CO₂ Utilization and Removal. *Nature* **2019**, *575*, 87–97.
- (2) Aresta, M.; Dibenedetto, A. Utilisation of CO₂ as a Chemical Feedstock: Opportunities and Challenges. *Dalton Trans* **2007**, 2975–2992.
- (3) Mikkelsen, M.; Jorgensen, M.; Krebs, F. C. The Teraton Challenge. A Review of Fixation and Transformation of Carbon Dioxide. *Energy Environ. Sci.* **2010**, *3*, 43–81.
- (4) Gibson, D. H. The Organometallic Chemistry of Carbon Dioxide. *Chem. Rev.* **1996**, *96*, 2063–2095.
- (5) Mascetti, J.; Galan, F.; Papai, I. Carbon Dioxide Interaction with Metal Atoms: Matrix Isolation Spectroscopic Study and DFT Calculations. *Coord. Chem. Rev.* **1999**, *190*, 557–576.
- (6) Armentrout, P. B. Reactions and Thermochemistry of Small Transition Metal Cluster Ions. *Annu. Rev. Phys. Chem.* **2001**, *52*, 423–461.
- (7) Walker, N. R.; Walters, R. S.; Duncan, M. A. Frontiers in the Infrared Spectroscopy of Gas Phase Metal Ion Complexes. *New J. Chem.* **2005**, *29*, 1495–1503.
- (8) Weber, J. M. The Interaction of Negative Charge with Carbon Dioxide - Insight into Solvation, Speciation and Reductive Activation from Cluster Studies. *Int. Rev. Phys. Chem.* **2014**, *33*, 489–519.
- (9) Dodson, L. G.; Thompson, M. C.; Weber, J. M. Characterization of Intermediate Oxidation States in CO₂ Activation. *Annu. Rev. Phys. Chem.* **2018**, *69*, 231–252.
- (10) Schwarz, H. Metal-Mediated Activation of Carbon Dioxide in the Gas Phase: Mechanistic Insight Derived from a Combined Experimental/Computational Approach. *Coord. Chem. Rev.* **2017**, *334*, 112–123.
- (11) Yanagimachi, A.; Koyasu, K.; Valdivielso, D. Y.; Gewinner, S.; Schoellkopf, W.; Fielicke, A.; Tsukuda, T. Size-Specific, Dissociative Activation of Carbon Dioxide by Cobalt Cluster Anions. *J. Phys. Chem. C* **2016**, *120*, 14209–14215.
- (12) Green, A. E.; Justen, J.; Schoellkopf, W.; Gentleman, A. S.; Fielicke, A.; Mackenzie, S. R. IR Signature of Size-Selective CO₂ Activation on Small Platinum Cluster Anions, Pt_n⁻ (n = 4–7). *Angew. Chem., Int. Ed.* **2018**, *57*, 14822–14826.
- (13) Qiao, B.; Wang, A.; Yang, X.; Allard, L. F.; Jiang, Z.; Cui, Y.; Liu, J.; Li, J.; Zhang, T. Single-Atom Catalysis of CO Oxidation using Pt₁/FeO_x. *Nat. Chem.* **2011**, *3*, 634–641.
- (14) Ye, R.; Hurlburt, T. J.; Sabyrov, K.; Alayoglu, S.; Somorjai, G. A. Molecular Catalysis Science: Perspective on Unifying the Fields of Catalysis. *Proc. Natl. Acad. Sci. U. S. A.* **2016**, *113*, 5159–5166.
- (15) Chakraborty, I.; Pradeep, T. Atomically Precise Clusters of Noble Metals: Emerging Link between Atoms and Nanoparticles. *Chem. Rev.* **2017**, *117*, 8208–8271.
- (16) Liu, J.-C.; Tang, Y.; Wang, Y.-G.; Zhang, T.; Li, J. Theoretical Understanding of the Stability of Single-Atom Catalysts. *Nat. Sci. Rev.* **2018**, *5*, 638–641.
- (17) Ross, M. B.; De Luna, P.; Li, Y.; Dinh, C.-T.; Kim, D.; Yang, P.; Sargent, E. H. Designing Materials for Electrochemical Carbon Dioxide Recycling. *Nat. Catal.* **2019**, *2*, 648–658.
- (18) Gregoire, G.; Duncan, M. A. Infrared Spectroscopy to Probe Structure and Growth Dynamics in Fe⁺(CO₂)_n Clusters. *J. Chem. Phys.* **2002**, *117*, 2120–2130.
- (19) Gregoire, G.; Brinkmann, N. R.; van Heijnsbergen, D.; Schaefer, H. F.; Duncan, M. A. Infrared Photodissociation Spectroscopy of Mg⁺(CO₂)_n and Mg⁺(CO₂)_nAr Clusters. *J. Phys. Chem. A* **2003**, *107*, 218–227.
- (20) Walters, R. S.; Brinkmann, N. R.; Schaefer, H. F.; Duncan, M. A. Infrared Photodissociation Spectroscopy of Mass-Selected Al⁺(CO₂)_n and Al⁺(CO₂)_nAr Clusters. *J. Phys. Chem. A* **2003**, *107*, 7396–7405.
- (21) Walker, N. R.; Walters, R. S.; Grieves, G. A.; Duncan, M. A. Growth Dynamics and Intracluster Reactions in Ni⁺(CO₂)_n Complexes via Infrared Spectroscopy. *J. Chem. Phys.* **2004**, *121*, 10498–10507.
- (22) Jaeger, J. B.; Jaeger, T. D.; Brinkmann, N. R.; Schaefer, H. F.; Duncan, M. A. Infrared Photodissociation Spectroscopy of Si⁺(CO₂)_n and Si⁺(CO₂)_nAr Complexes - Evidence for Unanticipated Intracluster Reactions. *Can. J. Chem.* **2004**, *82*, 934–946.
- (23) Ricks, A. M.; Brathwaite, A. D.; Duncan, M. A. IR Spectroscopy of Gas Phase V(CO₂)_n⁺ Clusters: Solvation-Induced Electron Transfer and Activation of CO₂. *J. Phys. Chem. A* **2013**, *117*, 11490–11498.
- (24) Xing, X.-P.; Wang, G.-J.; Wang, C.-X.; Zhou, M.-F. Infrared Photodissociation Spectroscopy of Ti⁺(CO₂)₂Ar and Ti⁺(CO₂)_n (n = 3–7) Complexes. *Chin. J. Chem. Phys.* **2013**, *26*, 687–693.
- (25) Iskra, A.; Gentleman, A. S.; Kartouzian, A.; Kent, M. J.; Sharp, A. P.; Mackenzie, S. R. Infrared Spectroscopy of Gas-Phase M⁺(CO₂)_n (M = Co, Rh, Ir) Ion–Molecule Complexes. *J. Phys. Chem. A* **2017**, *121*, 133–140.
- (26) Zhao, Z.; Kong, X.; Yang, D.; Yuan, Q.; Xie, H.; Fan, H.; Zhao, J.; Jiang, L. Reactions of Copper and Silver Cations with Carbon Dioxide: An Infrared Photodissociation Spectroscopic and Theoretical Study. *J. Phys. Chem. A* **2017**, *121*, 3220–3226.
- (27) Zimmermann, N.; Bernhardt, T. M.; Bakker, J. M.; Barnett, R. N.; Landman, U.; Lang, S. M. Infrared Spectroscopy of Gas-Phase Mn_xO_y(CO₂)_z⁺ Complexes. *J. Phys. Chem. A* **2020**, *124*, 1561–1566.
- (28) Knurr, B. J.; Weber, J. M. Solvent-Driven Reductive Activation of Carbon Dioxide by Gold Anions. *J. Am. Chem. Soc.* **2012**, *134*, 18804–18808.
- (29) Knurr, B. J.; Weber, J. M. Solvent-Mediated Reduction of Carbon Dioxide in Anionic Complexes with Silver Atoms. *J. Phys. Chem. A* **2013**, *117*, 10764–10771.
- (30) Knurr, B. J.; Weber, J. M. Infrared Spectra and Structures of Anionic Complexes of Cobalt with Carbon Dioxide Ligands. *J. Phys. Chem. A* **2014**, *118*, 4056–4062.
- (31) Knurr, B. J.; Weber, J. M. Structural Diversity of Copper-CO₂ Complexes: Infrared Spectra and Structures of Cu(CO₂)_n⁻ Clusters. *J. Phys. Chem. A* **2014**, *118*, 10246–10251.
- (32) Knurr, B. J.; Weber, J. M. Interaction of Nickel with Carbon Dioxide in Ni(CO₂)_n⁻ Clusters Studied by Infrared Spectroscopy. *J. Phys. Chem. A* **2014**, *118*, 8753–8757.
- (33) Thompson, M. C.; Ramsay, J.; Weber, J. M. Solvent-Driven Reductive Activation of CO₂ by Bismuth: Switching from Metalloformate Complexes to Oxalate Products. *Angew. Chem., Int. Ed.* **2016**, *55*, 15171–15174.
- (34) Thompson, M. C.; Ramsay, J.; Weber, J. M. Interaction of CO₂ with Atomic Manganese in the Presence of an Excess Negative Charge Probed by Infrared Spectroscopy of Mn(CO₂)_n⁻ Clusters. *J. Phys. Chem. A* **2017**, *121*, 7534–7542.
- (35) Kafafi, Z. H.; Hauge, R. H.; Billups, W. E.; Margrave, J. L. Carbon Dioxide Activation by Lithium Metal. 1. Infrared Spectra of Li⁺CO₂⁻, Li⁺C₂O₄⁻ and Li₂²⁺CO₂²⁻ in Inert-Gas Matrices. *J. Am. Chem. Soc.* **1983**, *105*, 3886–3893.
- (36) Kafafi, Z. H.; Hauge, R. H.; Billups, W. E.; Margrave, J. L. Carbon Dioxide Activation by Alkali Metals. 2. Infrared Spectra of M⁺CO₂ and M₂²⁺CO₂²⁻ in Argon and Nitrogen Matrices. *Inorg. Chem.* **1984**, *23*, 177–183.

(37) Miller, G. B. S.; Esser, T. K.; Knorke, H.; Gewinner, S.; Schoellkopf, W.; Heine, N.; Asmis, K. R.; Uggerud, E. Spectroscopic Identification of a Bidentate Binding Motif in the Anionic Magnesium-CO₂ Complex ([ClMgCO₂]⁻). *Angew. Chem., Int. Ed.* **2014**, *53*, 14407–14410.

(38) Jestila, J. S.; Denton, J.; Perez, E. H.; Khuu, T.; Apra, E.; Xantheas, S. S.; Johnson, M. A.; Uggerud, E. Characterization of the Alkali Metal Oxalates (MC₂O₄⁻) and Their Formation by CO₂ Reduction via the Alkali Metal Carbonites (MCO₂⁻). *Phys. Chem. Chem. Phys.* **2020**, *22*, 7460–7473.

(39) Barwa, E.; Pascher, T. F.; Oncak, M.; van der Linde, C.; Beyer, M. K. Carbon Dioxide Activation at Metal Centers: Evolution of Charge Transfer from Mg⁺ to CO₂ in [MgCO₂(H₂O)_n]⁺, n = 0–8. *Angew. Chem., Int. Ed.* **2020**, *59*, 7467–7471.

(40) Xie, H.; Wang, J.; Qin, Z. B.; Shi, L.; Tang, Z. C.; Xing, X. P. Octacoordinate Metal Carbonyls of Lanthanum and Cerium: Experimental Observation and Theoretical Calculation. *J. Phys. Chem. A* **2014**, *118*, 9380–9385.

(41) Zhao, Z.; Kong, X.; Yuan, Q.; Xie, H.; Yang, D.; Zhao, J.; Fan, H.; Jiang, L. Coordination-Induced CO₂ Fixation into Carbonate by Metal Oxides. *Phys. Chem. Chem. Phys.* **2018**, *20*, 19314–19320.